




## Testing the monophyly of the ground-dweller spider genus *Harpactea* Bristowe, 1939 (Araneae, Dysderidae) with the description of three new species

Leonardo Platania , Martina Pavlek & Miquel Arnedo

To cite this article: Leonardo Platania , Martina Pavlek & Miquel Arnedo (2020): Testing the monophyly of the ground-dweller spider genus *Harpactea* Bristowe, 1939 (Araneae, Dysderidae) with the description of three new species, Systematics and Biodiversity, DOI: [10.1080/14772000.2020.1776786](https://doi.org/10.1080/14772000.2020.1776786)

To link to this article: <https://doi.org/10.1080/14772000.2020.1776786>

 View supplementary material 

 Published online: 16 Jul 2020.

 Submit your article to this journal 

 View related articles 

 View Crossmark data 

## Research Article



# Testing the monophyly of the ground-dweller spider genus *Harpactea* Bristowe, 1939 (Araneae, Dysderidae) with the description of three new species

LEONARDO PLATANIA<sup>1\*</sup>, MARTINA PAVLEK<sup>2,3,4\*</sup>  & MIQUEL ARNEDO<sup>2</sup> <sup>1</sup>Institut de Biologia Evolutiva (CSIC-Universitat Pompeu Fabra), Passeig Marítim de la Barceloneta 37, Barcelona, 08003, Spain<sup>2</sup>Department of Evolutionary Biology, Ecology and Environmental Sciences, & Biodiversity Research Institute (IRBio) Universitat de Barcelona, Avinguda Diagonal 643, Barcelona, Spain<sup>3</sup>Croatian Biospeleological Society, Demetrova 1, Zagreb, 10000, Croatia<sup>4</sup>Ruder Bošković Institute, Bijenička 54, Zagreb, 10000, Croatia

The genus *Harpactea* Bristowe, 1939 (Araneae, Dysderidae) is one of the most diverse and abundant components of the Mediterranean ground-dwelling spider fauna. However, the taxonomic boundaries of the genus are unclear and its monophyly has been questioned, yet never tested, in a quantitative framework. The only taxonomic revisions in the genus trace back to the 1960s–1990s, and most subsequent work has consisted of single species descriptions. Part of the confusion surrounding the genus and species groups delimitations have to do with the lack of a standardized nomenclature for diagnostic structures based on explicit homology statements. Here we use the description of new species of *Harpactea* to propose a set of homologies in the male and female genitalia and a standardized nomenclature for those structures. We formally describe three new *Harpactea* species: *H. salvatorei* sp. nov., from a cave in the north-eastern Italian Alps, and *H. damini* sp. nov. and *H. mateparlovi* sp. nov. from different caves on the Biokovo Mountain and surroundings in Croatia. All the new taxa belong to the *lepida* species group. In addition, we use a multilocus target gene approach to provide the first hypothesis on the internal phylogenetic structure of the genus *Harpactea* and the subfamily Harpacteinae, which includes representatives of all currently accepted species groups in the genus and genera in the subfamily. Our results support the close affinities of the species here described but reject the monophyly of both *Harpactea* and some of the species groups proposed in the literature.

<http://zoobank.org/NomenclaturalActs/bd2739c9-c1f0-451f-88cc-06c784987a62>
<http://zoobank.org/NomenclaturalActs/ffb50b2e-ac7b-49a8-aa0d-408143c8a990>
<http://zoobank.org/NomenclaturalActs/184c58fe-6501-4cc2-ba50-cca4fcff8289>
**Key words:** Alps, caves, Dinarides, genitalic homologies, phylogeny, Sanger sequencing, taxonomy

## Introduction

Dysderidae Koch, 1837 is a highly diverse family of spiders of Western palearctic distribution, particularly abundant in the Mediterranean basin, where it is commonly found in ground habitats, especially leaf litter, and also often in caves. The family is one of the most species-rich lineages in the region and contributes to an important fraction of the European spider fauna (Chatzaki & Arnedo, 2006; World Spider Catalog, 2020). Dysderidae is currently divided into three subfamilies and 25 genera, with a very asymmetric distribution of species richness:

only two genera (*Dysdera* Latreille, 1804 and *Harpactea* Bristowe, 1939) make up 80% of the family diversity (World Spider Catalog, 2020). The genus *Harpactea* ranks second in the family in number of species, with 183 currently accepted (World Spider Catalog, 2020). The first complete revision of the genus was made by Alicata (1966), who separated the species in three phyletic groups based on the male genitalia (further divided into eight subgroups) that were suggested to deserve genus status, namely the *hombergi*-group, the *lepida*-group, and the *hedschi*-group. Based on the same set of characters, Brignoli (1978) divided the genus in two species groups – the *corticalis*-group and the *hombergi*-group – and ten subgroups. The last taxonomic treatment of the whole genus was conducted by Deeleman-Reinhold (1993).

Correspondence to: Miquel Arnedo. E-mail: [marnedo@gmail.com](mailto:marnedo@gmail.com)

\*These authors contributed equally to the paper

Unlike former delimitations, she mostly relied on female genital structures (posterior diverticulum) and organized the genus in four groups: the *corticalis*-group, the *hombergi*-group, the *lepida*-group, and the *rubicunda*-group. More recently, Le Peru (2011) grouped 74 *Harpactea* species into 14 groups solely based on the general resemblance of the embolic division of the male palp, without providing further justification. Because all former subgeneric circumscriptions were based on overall similarity (i.e., phenetic approximations) neglecting homology statements and evolutionary history of the group, none of them can be considered completely satisfactory. Moreover, the genus boundaries are also problematic. In its present circumscription, *Harpactea* is better considered as a mix of three-clawed species that do not fit any of the more narrowly defined genera within the subfamily Harpacteinae (Chatzaki & Arnedo, 2006). The monophyly of the genus has been repeatedly questioned, even by the same authors proposing the species groups. For example, in her proposal of species groups Deeleman-Reinhold suggested that the *rubicunda* group was more closely associated to species in the genus *Dasumia* Thorell, 1875 and *Stalagtia* Kratochvil, 1970, implicitly assuming that the group was paraphyletic. To date, neither the monophyly nor the internal structure of the genus have been subject to a rigorous evaluation using a quantitative phylogenetic framework.

The conflict in defining both the internal organization and the delimitation of the genus stems from the fact that little effort has been done to assess homology among the main morphological characters. As observed in other dysderids, *Harpactea* is highly uniform in somatic morphology. Most species diagnostic characters are restricted to the male genitalia, while female genitalia mostly defines species groups. In the specific case of the copulatory bulb, different authors have used different terms to refer to the same structures (Alicata, 1966; Deeleman-Reinhold, 1993), or have even avoided referring to the structures with any specific name (e.g. Gasparo, 2013). Standardizing the terminology of the diagnostic traits based on well-founded homology statements is an unavoidable task to resolve the taxonomic turmoil surrounding *Harpactea*, and will provide the basis for delimiting taxonomic groups in a proper evolutionary framework.

Despite the wide distribution of the genus that stretches from Portugal to Turkmenistan, most species are narrow endemics and only few are widespread (Bosselaers & Van Keer, 2016) – e.g., *H. hombergi* (Scopoli, 1763), *H. lepida* (C.L. Koch, 1838), *H. rubicunda* (C.L. Koch, 1838) and *H. saeva* (Herman, 1879). The checklist of the spider fauna of Italy currently includes 21 *Harpactea* species (Pantini & Isaia, 2019). The araneophauna of the north-eastern region of Italy is

well-studied (Ballarin *et al.*, 2011), including the cave dwelling spiders (Roewer, 1931; Gasparo & Thaler, 2000). The Croatian spider fauna, on the other hand, is much less known. It currently includes only five *Harpactea* species, four widespread and one endemic (Nentwig *et al.*, 2020; Rucner & Rucner, 1995), all of them epigeal. The Balkan region is, overall, very rich in *Harpactea* species with 56 species currently recorded (Deltshev & Lazarov, 2018; Lazarov & Dimitrov, 2018; Dimitrov *et al.*, 2019), 45 of which are Balkan endemics (Nentwig *et al.*, 2020).

In this article, we propose a standardized terminology of the *Harpactea* genitalia, based on explicit homology statements, and describe three new species, one collected from a cave in the Italian north-eastern Alps (Barcis, PN), and two from different caves on the Biokovo Mountain and surroundings in Croatia. In addition, we use a multilocus target gene approach to infer a preliminary hypothesis of the phylogenetic structure of the genus *Harpactea*, which supports the close affinities of the species here described and rejects the monophyly of the genus and of some of the species groups proposed in the literature.

## Materials and methods

### Morphological studies

The specimens from Italy were sampled with pitfall traps containing water saturated with NaCl and then conserved in 75% ethanol. The specimens from Croatia were hand collected, if not stated otherwise, and conserved in 70 or 96% ethanol. After removal from opisthosoma, the vulvas were treated with 30% KOH for 5–10 minutes, washed in distilled water and stored in ethanol.

Morphological observations were carried through stereo microscope Leica MZ16 A equipped with digital camera Leica DFC450, Zeiss Stereo Discovery V12 stereo microscope with Canon EOS 80 D digital camera, optical microscope Leitz DMRB with ProgRes C3 coll camera, and by Q-200 (FEI Co.) scanning electron microscope (SEM). For the SEM images the samples were sonicated for roughly 30 s with ultrasonic laboratory bath Nahita ZCC001, dehydrated through immersion in increasing dilutions of ethanol (80%, 85%, 90%, 100%) and carbon coating. All measurements are in millimetres (mm).

The definition and terminology of genital structures used in *Harpactea* descriptions has been summarized in Deeleman-Reinhold (1993) and Chatzaki and Arnedo (2006). However, because of the confusion around the terminology and, most importantly, about the homology

of some of the structures that has traditionally plagued *Harpactea* taxonomy, it is essential to provide a clear and explicit definition and a standardized terminology of homologous genitalic structures. To facilitate comparison and to improve objectivity we will use the terms listed in the spider anatomy ontology (SPD) recently proposed by Ramírez and Michalik (2019), including their ID codes. Dysderids in general and *Harpactea* in particular, show a wide range of variation in the morphology and complexity of the male copulatory bulb (SPD:0000168), and establishing homology across the different structures is challenging. A common pattern to all the species is that the basal division (SPD:0000521) is reduced, almost invisible, and the most conspicuous structures are those of the median (SPD:0000522) and embolic (SPD:0000175) divisions (e.g., Figs 30, 31, 32). The median division is mostly formed by a subspheric to elongated ovoid tegulum (SPD:0000173). The tegulum connects to the cymbium (SPD:0000158) through a membrane, probably the remnants of the basal (SPD:0000170) and/or median (SPD:0000174) hematochae. A recurrent problem when illustrating male palps is the actual orientation. The relative position of the copulatory bulb in relation to the cymbium may change. Therefore, referring to the position of the different structures in the copulatory bulb in relation to the position of the cymbium (e.g., retrolateral, prolateral) may be misleading. Fortunately, the subequal shape of the tegulum and its subbasal insertion to the cymbium, provide an alternative reference system in *Harpactea*. Here we propose to arbitrarily define the side where the tegulum connects to the cymbium as internal. The internal side of the tegulum is usually expanded towards its base (distally), before a constriction after which the tegulum flattens distally. On the external side, the shape of the tegulum is semicircular, with no expansion or dilation towards the distal constraint. The tegulum may bear some projections in the form of apophyses. Since these apophyses are actually fused to the tegulum, they are better considered as homologous to the median (SPD:0000178) and paramedian apophysis (SPD:0000707). In the species of the *lepida* group (see below) a well-developed apophysis, situated right below the basal expansion and projected retro-laterally, is most evident. We will arbitrarily refer to this structure as the median apophysis (see above). Some species (e.g., *H. grisea* (Canestrini, 1868)) bear a second tegular apophysis located at the distal part of the flattened area of the tegulum. We will refer to this structure as the paramedian apophysis (see above). In the frontal side of the flattened distal part of the tegulum there is a membranous area with additional outgrowths and projections that we interpret as the embolic division (SPD:0000175). We

suggest that the membranous area corresponds to the terminal haemethodoca (SPD:0000180). The interpretation of the apophyses, however, is more challenging. The unambiguous identification of the embolus (SPD:0000176) generally requires locating the sperm outlet (SPD:0000269) to confirm the internal presence of the spermophor (SPD:0000177), which may be difficult even when SEM images are available. In general, the embolus seems to grow from the external side of the embolic division. The embolus shape varies, ranging from a fully sclerotized, tube-like apophysis to a flattened structure bearing membranous expansions. A second apophysis, which may also adopt a variety of forms and have different levels of development, generally accompanies the embolus and is usually located at its internal side. Because of its close association to the tegulum, we here refer to the second apophysis of the embolic division as the conductor (SPD:0000179).

The female genitalia of *Harpactea* has been studied in detail by Burger & Kropf (2007). The epigastric furrow (SPD:0000034) opens into an internal pouch, the bursa (SPD:0000280), which divides into an anterior section (SPD:0000553), and a posterior diverticulum (SPD:0000283), the last being a synapomorphy of the Dysderoidea superfamily (Forster & Platnick, 1985). In the group *lepida*, the posterior diverticulum is usually wider than long and bears a lightly chitinized button at its distal end (Deeleman-Reinhold, 1993), the receptaculum (Burger & Kropf, 2007) (Fig. 37). A series of gland cells are connected to the receptaculum. The anterior dorsal part of the posterior diverticulum is heavily sclerotised, the transversal bar, and bears a lamella that articulates with the posterior border of the anterior section of the genitalia, which is also sclerotized and has an inverted T shape (Figs 36–38). This lock system forms the uterine valve (SPD:0000586), which regulates the pass between the uterus externus (SPD:0000591) and the uterus internus (SPD:0000591), which continues into the oviduct (SPD:0000772), by the action of the muscles attached to the sclerotized dorsal margins of the posterior diverticulum and the anterior section. The anterior section is heavily sclerotized and bears a stalk-like sclerite projected forwards with a strongly thickened distal part, and two roundish structures (RS) at both sides of the base of the stalk (Fig. 37). The stalk-like sclerite serves as muscle attachment. Burger & Kroof reported the presence of spermatozoa in the posterior diverticulum, the roundish structures and the receptaculum, but not in the stalk-like sclerite, although this structure is apparently hollow. Interestingly, in the taxonomic literature most authors have traditionally referred to the stalk-like apophysis as the spermatheca (S) (SPD:0000699).

## Abbreviations

*Prosona*: CL: carapace length, CWmax: maximum carapace width, CWmin: minimum carapace width, SL: sternum length. *Opisthosoma*: OL: opisthosoma length. *Chelicerae*: ChF: length of cheliceral fang, ChG: length of cheliceral groove, ChL: total length of chelicera (lateral external view), PT: promarginal teeth, RT: retromarginal teeth. *Eyes*: AME(d): anterior median eyes (diameter), PLE(d): posterior lateral eyes (diameter), PME(d): posterior median eyes (diameter). *Legs*: Cx: Coxa, Fe: femur, Me: metatarsus, Pa: patella, Ta: tarsus, Ti: tibia, pl: prolateral, rl: retrolateral. *Male copulatory bulb*: C: conductor, E: embolus, o: sperm outlet, MA: median apophysis, PA: paramedian apophysis, T: tegulum. *Vulva*: AC: anterior arc (anterior section), PD: posterior diverticulum, R: receptaculum, RS: roundish structures, S: spermatheca, SK: spermathecal keel, TB: transversal bar.

## Collection abbreviations

CBSS: Croatian Biospeleological Society, Zagreb, Croatia; FG: Fulvio Gasparo personal collection, Trieste, Italy; MCNB: Museu de Ciències Naturals de Barcelona, Catalonia, Spain; MCSNB: Museo Civico di Scienze Naturali 'E. Caffi', Bergamo, Italy.

## Taxonomic sampling

At least one representative of each of the Harpacteinae genera, the type species when possible, as well as of the *Harpactea* species groups proposed by Deeleman-Reinhold (1993) were included in the analyses. Available sequences of dysderids from former studies (Arnedo *et al.*, 2001, 2007, 2009; Astrin *et al.*, 2016; Bidegaray-Batista, Macías-Hernández, Oromí, & Arnedo, 2007; Bidegaray-Batista & Arnedo, 2011; Bidegaray-Batista *et al.*, 2014; Macías-Hernández *et al.*, 2008, 2010; Wheeler *et al.*, 2017) were obtained from GenBank. Additional sequences were obtained for two of the new species here described. None of the specimens of *H. salvatorei* sp. nov. yielded DNA of high enough quality for amplification, probably as a result of the collection method. Specimens information and accession numbers are available at Table S1.

## Molecular procedures

Total genomic DNA was extracted from leg tissue using two different commercial kits: Speedtools Tissue DNA Extraction Kit (Biotools) as general extraction procedure, and QIAamp DNA Micro Kit (Qiagen), which provides a more sensitive extraction, for older and worse

preserved samples. DNA fragments of five genes were targeted for the present study, the mitochondrial genes encoding cytochrome c oxidase subunit I (COI) and ribosomal RNA 16S, and the nuclear genes for histone H3 and ribosomal RNA 28S and 18S. DNA amplifications were carried out in a 20 µl reaction volume, including 5 µl of MyTaq Red Reaction Buffer from Bioline; which contains the four types of dNTPs (5 mM), MgCl<sub>2</sub> (15 mM), stabilizers and enhancers; 0.2 µl of both forward and reverse 0.1 M primers, 0.2 µl of MyTaq Red DNA Polymerase from Bioline, 2–4 µl of genomic DNA (depending on the quality of the sample) and ultrapure Milli-Q water to make up the final volume. The information of the primers used in the amplification and subsequent sequencing of the different gene regions are available at Table S2 and the profiles for the PCR amplifications in Table S3. Unpurified PCR products were sent to the Macrogen services, and were sequenced in both directions by Sanger method, using the same primers as for amplification. Sequence chromatograms for both directions of each sample were assembled, checked and edited using Geneious v. 8.1.9 (Kearse *et al.*, 2012).

## Phylogenetic analyses

The ribosomal genes were automatically aligned using the Geneious plugin of the alignment program MAFFT v. 7.017 (Katoh *et al.*, 2002) using default options. All genes were concatenated in a super matrix for subsequent phylogenetic analyses. The concatenated matrix has 47 terminals, 1010 bp of the COI, 625 aligned positions of the 16S, 329 bp of the H3, 811 bp of the 18S, and 795 aligned positions of the 28S.

Parsimony analysis of the matrix was conducted with the program TNT v1.5 (Goloboff & Catalano, 2016). The search strategy consisted of 1000 Wagner trees built with random addition of taxa and subsequent TBR branch swapping. Branches where minimum possible length in any most parsimonious reconstruction was zero, were removed from final trees. Support values were estimated by jackknifing frequencies, with a probability of character removal set to 0.33, derived from 1000 resampled matrices using 20 random addition sequences, and retaining 5 trees per replication, followed by TBR and TBR collapsing to calculate the consensus. The best Maximum likelihood tree was inferred with IQ-TREE v. 1.6.9 (Nguyen *et al.*, 2015). We used ModelFinder to first select the best-fit partitioning scheme and corresponding evolutionary models (Kalyaanamoorthy *et al.*, 2017), and then to infer the best tree and estimate clade support by means of 1000 replicates of standard non-parametric bootstrapping.



Bayesian inference was implemented with MrBayes v3.2.6 (Ronquist & Huelsenbeck, 2003). The best partition scheme and corresponding model was first assessed with the help of the program Partition Finder v2.1.1 (Lanfear et al., 2017). The analysis was run for 15 million generations, sampling each 1000, with eight simultaneous Markov chain Monte Carlo (MCMC) chains, 'heating temperature' of 0.15, and a relative initial burn-in of 25%. Support values were calculated as posterior probabilities. Convergence of the chains, correct mixing and the number of burn-in generations were monitored with Tracer v. 1.7 (Rambaut et al., 2018). Model based analyses were run remotely at the CIPRES Science Gateway (Miller et al., 2010). The phylogenetic tree was edited for aesthetic purposes using FIGTREE (<http://tree.bio.ed.ac.uk/software/figtree/>).

## Results

### Taxonomy:

**Family Dysderidae** C. L. Koch, 1837

**Genus *Harpactea*** Bristowe, replacement name for *Harpactes* Templeton, 1835, preoccupied, provided by Bristowe, 1939: 5 (see Roewer, 1955c: 1715).

Type species: *Harpactea hombergi* (Scopoli, 1763), by original designation.

***Harpactea salvatorei*** sp. nov. Platania & Arnedo (Figs 1–14)

**Type specimens.** HOLOTYPE: 1♂ Italia, Friuli-Venezia Giulia, Barcis (PN) Grotta della Vecchia Diga, 46.18°N, 12.17°E, 17.V.2006, leg. G. Trezzi. Deposited at MCSNB. PARATYPES: 1♀ 1♂ Italia, Friuli-Venezia Giulia, Barcis (PN) Grotta della Vecchia Diga, 46.18°N, 12.17°E, 17.V.2006, leg. G. Trezzi. Deposited at MCSNB.

**Type locality.** Italia, Friuli-Venezia Giulia, Barcis (PN), Grotta della vecchia diga, (cadastral number 786RE/327Fr). This cave at 483 m of altitude and with a length of 1388 m, was discovered in 1952 and was already the object of speleological and biospeleological studies (Corrado, 1953; Mosetti, 1954a, 1954b; Belloni et al., 1971; Grottolo, 1994; Gasparo, 1997; Piva, 2005).

**Other material examined.** *H. grisea* (Canestrini, 1868): Italia, Friuli-Venezia Giulia, Villa Santina (UD), m 400, carpineto, 11.II.-29.IV.1994, leg. F. Gasparo. FG

collection. *H. tergestina* Gasparo, 2013: Italia, Friuli-Venezia Giulia, Prosecco, m 240, prov. Trieste, 1.X.-1.XI.1991, leg. F. Gasparo. FG collection.

**Etymology.** Named in honour of Salvatore Platania, LP's father, who taught him since his early years to observe and love nature and all forms of living beings, and continues to be a reference and a source of inspiration. Furthermore, this species was discovered exactly on the day of his 60th birthday, while waiting for the celebration party. The name is in genitive.

**Diagnosis.** The species closely resembles *H. tergestina* and *H. grisea* by the presence of a dorsal process in the palp Pa (Fig. 4). It can be distinguished from the former species by MA rectangular shape (Figs 5–8): flat in *H. salvatorei* sp. nov., bifid in *H. tergestina*, Y-shaped in *H. grisea*; E shape: laminar in *H. salvatorei* sp. nov., with a basal row of teeth in *H. tergestina*, slender, curved, pointed in *H. grisea* (Figs 9, 11, 12). Female genitalia of *H. salvatorei* sp. nov. differs from the other species by a short, polygonal spermatheca (Figs 13–14), remarkably longer in both *H. grisea* and *H. tergestina*.

**Description.** Male holotype. Measurements: CL, 2.954; Cwmax, 2.315; Cwmin, 0.91; OL, 3.2; ChL, 1.34; ChG, 0.33; ChF, 0.93; AMEd, 0.14; PLEd, 0.1; PMEd, 0.09. Carapace (Fig. 1) with smooth surface, orange to light brown, darker along the border. Thoracic region with a polygonal contour, posterior border straight and slightly concave. A few long setae in front of the ocular area region, the rest of carapace almost glabrous. Fovea barely visible, longitudinal. Posterior eyes recurved, relative eye size AME > PLE > PME; AME separated by ~1/2 their diameter, PLE from the others by less, PME adjacent. Clypeus height 0.07. Sternum (Fig. 2) shiny, 1.83 long, same colour as carapace with scarce setae in the middle and quite copious and long on the external region, along the perimeter. Labium length 0.56, width 0.29. Chelicerae (Fig. 3) same colour as frontal part of prosoma; cheliceral groove armed with 5 small teeth of similar size (0.02 width, 0.03–0.02 height), two on the promargin, positioned proximally and almost touching each other. Two on the retromargin separated by 0.25, one more tooth distally positioned in the retromargin, approximately at a half the distance between the two basal teeth and the fang insertion. Cheliceral groove dorsally covered with long setae, arranged in two lines. Opisthosoma pale green yellowish uniform dorsoventrally. Spinneret morphology is highly conserved across dysderids, other than reduction in the number of spigots in highly adapted cave-dwelling



**Figs. 1–4.** *Harpactea salvatorei* sp. nov. male habitus. 1. Prosoma, dorsal view; 2. Prosoma, ventral view; 3. Chelicerae, ventral view; 4. Left palp, retrolateral view. Scale bars = 1 mm (1, 2, 4); 0.5 mm (3). Abbreviations: PT, promarginal teeth; RT, retromarginal teeth.

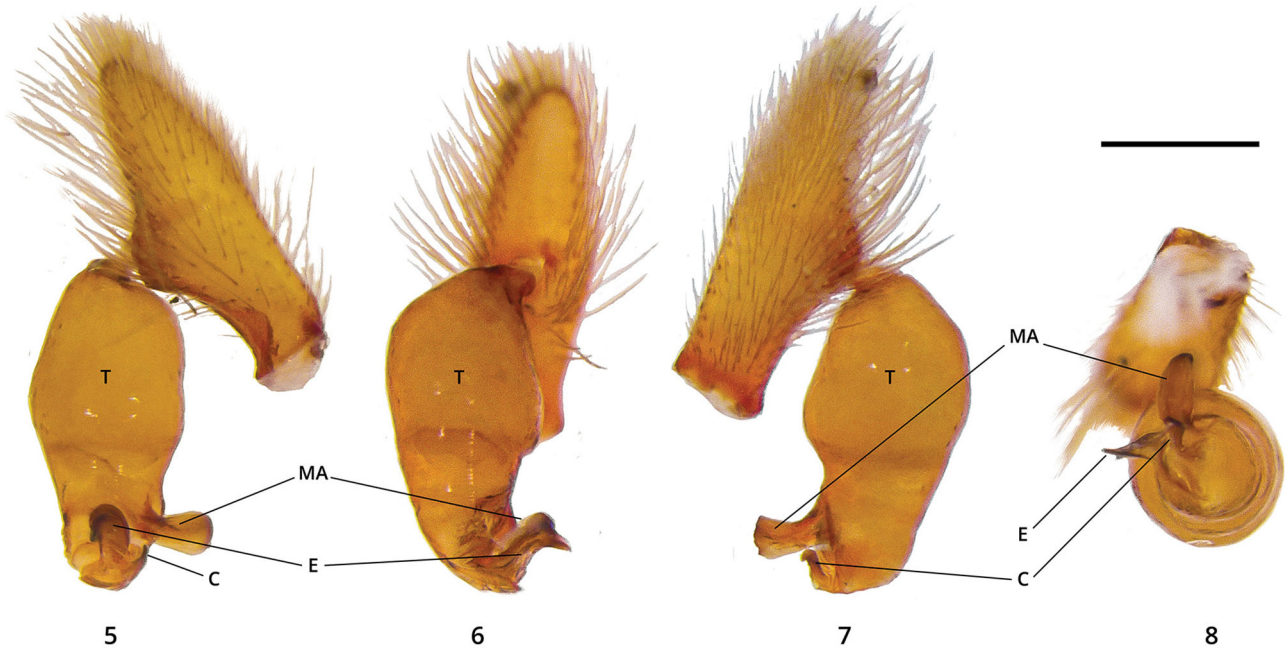
species (Arnedo *et al.*, 2007), and hence spinnerets of the new species here described were not illustrated.

Leg measurements: Fe I, 2.99; Fe II, 2.62; Fe III, 2.14; Fe IV, 2.88; Pa I, 1.92; Pa II, 1.66; Pa III, 1.3; Pa IV, 1.31; Ti I, 2.59; Ti II, 2.17; Ti III, 1.69; Ti IV, 2.49; Mt I, 2.55; Mt II, 2.26; Mt III 3.05; Mt IV, 3.11; Ta I, 0.82; Ta II, 0.77; Ta III, 0.94; Ta IV, 0.92. All legs coloured as the carapace, anterior pairs darker, Ta with 3 claws. Relative leg length:  $I > IV > II > III$ . Spines present on all Fe and the posterior Ti and Ta; all Cx, Pa and Ta spineless. Fe I and II with 5 pd spines distally clustered. Fe III with 7–8 dorsal spines arranged

in two longitudinal rows stretching along the whole length, the same disposition followed in Fe IV with 5–6 spines. Posterior Ti and Me with 10–11 and 14–16 spines respectively, distributed all along the segments.

Palp orange-brown as the other appendages (Fig. 4). Fe in the proximal part slightly curved outward, other segments straight, Pa with a conical dorsal process on the anterior 2/3, visible in lateral view, Ti straight, Ta triangular on lateral view. Copious pubescence on the distal segments – scarce on Fe and getting denser towards Ta which is covered by dense short setae dorsally and longer setae ventrally. Fe 1.3 long, Pa and Ta





**Figs. 5–8.** *Harpactea salvatorei* sp. nov. male bulb. 5. Prolateral view; 6. Frontal view; 7. Retrolateral view; 8. Ventral view. Scale bar = 0.3 mm. Abbreviations: C, conductor; E, embolus; MA, median apophysis; T, tegulum.

1/2 and  $T_i \sim 2/3$  of Fe length. Ratio  $T_i/T_a$  1.1. Proximal segments around 0.4 in diameter in the whole length, the distal segments around 0.2 in diameter.

Male copulatory bulb T piriform and asymmetric (Figs 5–8), 0.69 long at its longest point, on the proximal third, and 0.32 wide at the widest point (bulge). E is emerging from the outer rim of the membranous part (Figs 9–10). Is formed by a short lamina concave curved ahead projected to the prolateral side with basal laminar structures and a styliform arcuated process. MA is located at 2/3 of retrolateral face of T as a rectangular laminar process, feebly arcuated on the posterior direction, with a slight constriction on the basal part of the border that give it a tongue shape (Figs 5, 7); the distal border is flat, slightly convex and the anterior part is concave like a spoon. Finally, a short, laminar, quite flat and poorly visible C emerges from the middle of the membranous part, on the top of the structure, between the MA and E. On ventral view (Figs 8, 10), C is shaped as a curved bilobed spiralized and collapsed structure as a hood, resembling in shape the upper beak of a parrot. MA and C are directed posteriorly, E is directed retrolaterally.

Female paratype. Measurements: CL, 2.671; Cwmax, 2.004; Cwmin, 0.9; OL, 3.09; ChL, 1.26; ChG, 0.4; ChF, 0.58; AMEd 0.14; PLEd, 0.1; PMEd, 0.09. Leg measurements of paratype (♀): Fe I, 2.4; Fe II, 2.16; Fe III, 1.83; Fe IV, 2.58; Pa I, 1.53; Pa II, 1.4; Pa III 0.86, Pa IV 1.19; Ti I, 2.07; Ti II, 1.88; Ti III, 1.5; Ti IV, 2.16; Mt I, 1.99; Mt II, 1.92; Mt III, 1.83; Mt IV, 2.68;

Ta I, 0.67; Ta II 0.63; Ta III 0.66; Ta IV, 0.88. Somatic characters as in male, except labium length 0.46 width 0.31; clypeus height 0.1; relative leg lengths:  $IV > I > II > III$ .

Vulva is poorly sclerotized and simple in the general structure; there are no evident differences between the dorsal and ventral faces. AC straight in the transversal component, with tapering lateral edges on a dorsal view, which appear more regular and roundish on a ventral view; S reduced and short, horseshoe shaped, creating an arch on the bottom of the anterior arch; on a dorsal view is visible a polygonal border with a very little apophysis as an acute angle in the centre that is probably a reduced SK; TB similar in length to AC, a bit shorter and poorly sclerotized. PD and R poorly sclerotized, as visible in Figs 13–14, PD as wide as TB, R polygonal and feebly chitinized, as wide as S.

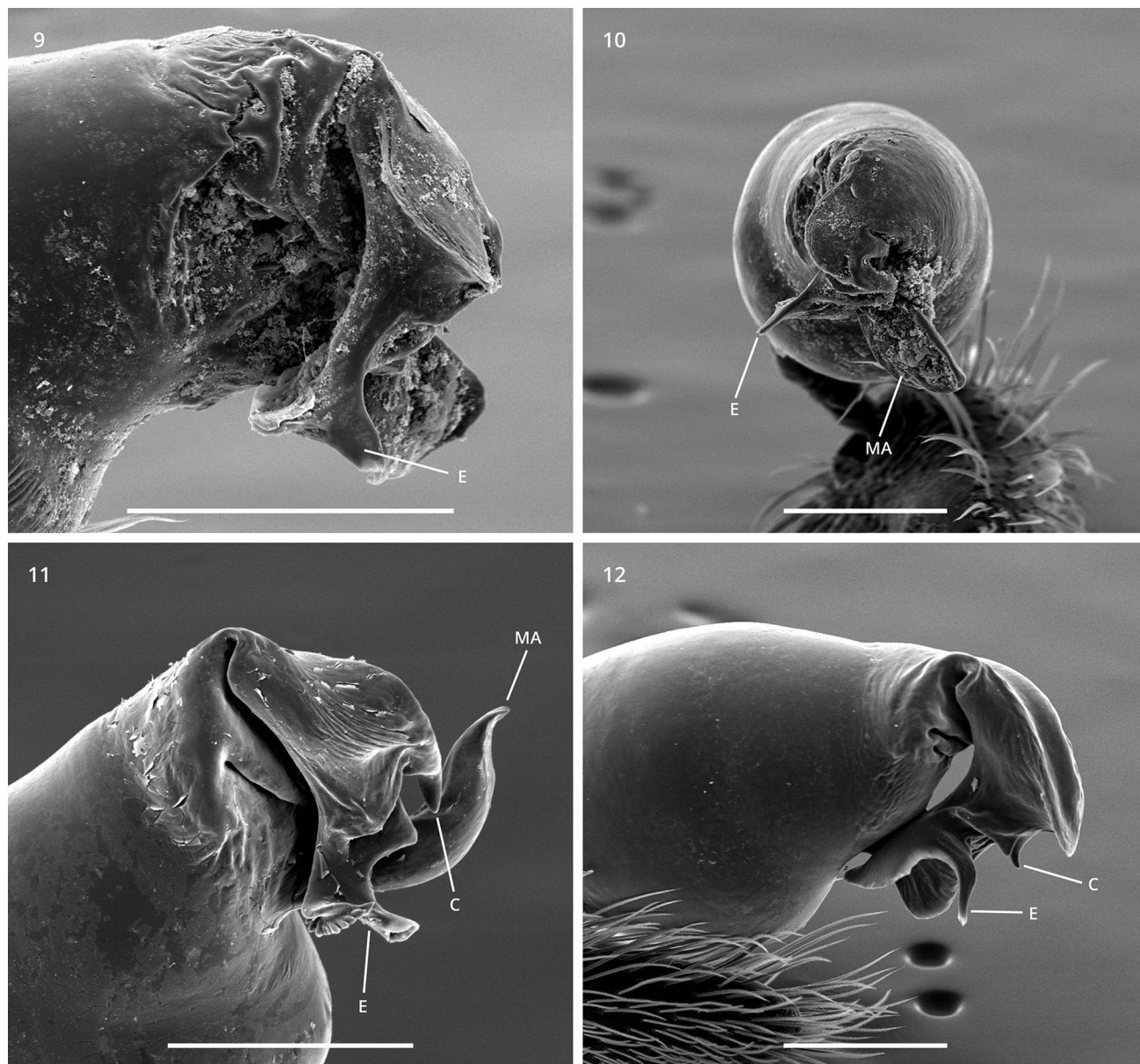
**Distribution.** Known only from the type locality, a cave in the Dolomites (Fig. 40).

*Harpactea damini* Pavlek & Arnedo sp. nov.  
(Figs 15–26)

**Synonyms.** *Harpactea* sp. – Mammola et al., 2019.

**Type specimens.** HOLOTYPE: 1♂ CBSS/AR 3919-1, Croatia, Biokovo Mtn, Jujnovića špilja, 43.26°N, 17.19°E, 29.IV.2014, leg. Branko Jalžić & Petra





**Figs. 9–12.** *Harpactea salvatorei* sp. nov., close-up with SEM microscope of apical structures of the male bulb and comparison with *H. tergestina* and *H. grisea*. 9. *H. salvatorei* sp. nov., prolateral view; 10. *H. salvatorei* sp. nov., ventral view. 11. *H. tergestina*, prolateral view; 12. *H. grisea*, prolateral view. Scale bar = 0.2 mm. Abbreviations: C, conductor; E, embolous; MA, median apophysis; T, tegulum.

Bregović (pitfall trap, NaCl). Deposited at CBSS. PARATYPES: 1♀ CBSS/AR 4293-1, 14.V.2016, leg. Alen Kirin; 1♀ CBSS/AR 1925-1, 14.X.2002, leg. Christa Deeelman-Reinhold; 1♀ CBSS/AR 3916, 29.IV.2014, leg. Branko Jalžić & Petra Bregović (pitfall trap, NaCl) – all three samples from the type locality. 1♂ CBSS/AR 1954, Croatia, Biokovo Mtn, Kukor, 43.35°N, 16.99°E, 26.IV.2002, leg. Roman Ozimec. 1♀ CBSS/AR 2368, Croatia, Mosor Mtn, Drinovčusa, HR02324, 43.54°N, 16.63°E, 21.VI.2011, leg. Petra

Bregović. 1♀ CBSS/AR 5473, Croatia, Biokovo Mtn, Samogorska špilja, HR00262, 43.31°N, 17.12°E, leg., 23.VI.2017, leg. Roman Ozimec. 1♂ CBSS/AR 4398-1, Croatia, Biokovo Mtn, Gradska spila, HR00362, 43.31°N, 17.11°E, 15.V.2016., leg. Anđela Čukušić. All samples above deposited at CBSS. 1♂ MZB 2019-2013, leg. Tin Rožman & 1♀ MZB 2019-2014, leg. Nikolina Kuharić, collection data for both samples: Croatia, Biokovo Mtn, Gradska spila, HR00362, 43.31°N, 17.11°E, 15.V.2016. Deposited at MCNB.

**Other material examined.** 1 juv ♂ CBSS/AR 1925-2, 14.X.2002, leg. Christa Deeleman-Reinhold, 3 juv CBSS/AR 3919-2, 29.IV.2014, leg. Branko Jalžić & Petra Bregović (pitfall trap, NaCl); 1 juv CBSS/AR 4293-2, 14.V.2016, leg. Alen Kirin – all from the type locality. 1 juv CBSS/AR 3911, 15.X.2014, leg. Peter Hlaváč & Jan Lakota; 1 juv CBSS/AR 3918, 1.V.2014, leg. Peter Hlaváč, Jan Lakota & David Čeplik – both from Croatia, Biokovo Mtn, Spila 1, 43.26°N, 17.20°E. 2 juv CBSS/AR 3917, 29.IV.2014, leg. Branko Jalžić & Petra Bregović; 1 juv CBSS/AR 4406, 14.V.2016, leg. Anđela Čukušić – both from Croatia, Biokovo Mtn, Spila 2, HR00263, 43.26°N, 17.20°E, 29.IV.2014. 1 juv CBSS/AR 4398-1, Croatia, Biokovo Mtn, Gradska spila, 15.V.2016., leg. Anđela Čukušić. 1 juv CBSS/AR 4514, Croatia, Biokovo Mtn, Stonjska peč donja, HR00264, 43.32°N, 17.13°E, 1.V.2012, leg. Martina Pavlek. All samples above deposited at CBSS.

**Type locality.** Croatia, Biokovo Mtn, Jujnovića špilja, cadastral number HR00363. Jujnovića špilja is a relatively small cave, 108 m long and 16 m deep, it's already a type locality for a pselaphine beetle *Thaumastocephalus slavkoi* Hlaváč et al., 2019.

**Etymology.** The species is named after Narcis Damin (1845–1905), the first dedicated Croatian arachnologists. He published the first complete spider checklist of present-day Croatia and formed the largest collection of spider specimens from Croatia, deposited in the Croatian Natural History Museum in Zagreb.

**Diagnosis.** It differs from all other *lepida* group species, including geographically closest *H. mateparlovi* sp. nov., *H. complicata* Deltšev, 2011 and *H. tenuimboli* Deltšev, 2011, by male bulb with thin, simple, rod shaped MA, with non-bifurcated tip (Figs 18–20). PA absent; E flat, broad, partly membranous on the edges (Figs 18–19); C slender, with hook shaped tip in lateral view, positioned between MA and E (Figs 18–23); MA, C, E similar in length, directed away from palp. Vulva AC with bifurcated lateral edges (Fig. 26); S with triangular base, transparent dorso-frontal SK on oval tip; R small, poorly sclerotized, round-shaped (Figs 24–26).

**Description.** Male holotype. Measurements: CL, 2.73; Cwmax, 2.05; Cwmin, 1.18; OL, 3.04; ChL, 1.22; ChG, 0.42; ChF, 0.62; AMEd, 0.12; PLEd, 0.1; PMEd, 0.09. Carapace (Fig. 15) with smooth surface, orange to light brown, darker in the front part. Outline polygonal with straight posterior border. Scarce setae in eyes region and on the posterior carapace edge. Fovea visible, longitudinal. Posterior eyes recurved, relative eye size

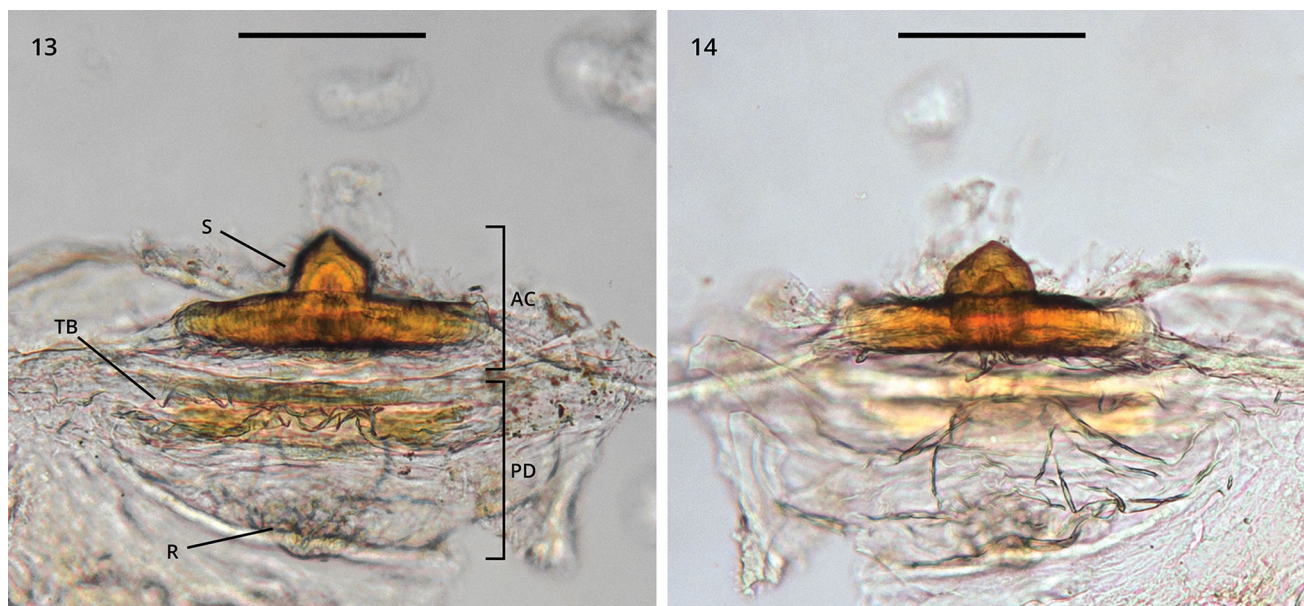
AME > PLE > PME; AME separated by  $\sim 1 \times$  their diameter, others by less. Clypeus height 0.09 mm. Sternum shiny, 1.95 mm long, same colour as carapace with scarce short setae (Fig. 16). Labium length 0.64, width 0.34 mm. Chelicerae same colour as frontal carapace; cheliceral groove armed with 4 teeth of similar size (0.33 width, 0.45 height). Two on the promargin, positioned proximally and almost touching each other. Two on the retromargin separated by 0.5 mm. Proximal-most retromarginal tooth distal to distal-most promarginal tooth and separated from it by 0.3 mm (Fig. 17). Cheliceral groove dorsally covered with long setae, arranged in two lines. Opisthosoma light grey.

Leg measurements: Fe I, 2.8; Fe II, 2.59; Fe III, 2.06; Fe IV, 2.7; Pa I, 1.92; Pa II, 1.64; Pa III, 1; Pa IV, 1.22; Ti I, 2.56; Ti II, 2.32; Ti III, 1.58; Ti IV, 2.43; Mt I, 2.48; Mt II, 2.22; Mt III 2.06; Mt IV, 2.91; Ta I, 0.64; Ta II, 0.63; Ta III, 0.63; Ta IV, 0.74. All legs dark yellow. Ta with 3 claws. Relative leg length: I > IV > II > III. Spines present on all Fe and the posterior Ti and Ta; all Cx, Pa and Ta spineless. Fe I and II with 4–6 pl spines distally clustered. Fe III and IV with 7–10 dorsal spines arranged in two longitudinal rows stretching along the whole length. Posterior Ti and Me with 14–17 and 11–15 spines respectively, distributed all along the segments.

Palps the same colour as legs (Figs 15–16). Fe in the proximal part slightly curved outward, other segments straight, Ta triangular in lateral view. Setae present on all segments – scarce on Fe and getting denser towards Ta which is covered by dense short setae dorsally and longer setae ventrally. Fe 1.09 mm long, Pa and Ta 0.55 and Ti 0.66. All segments 0.22–0.24 in diameter in the whole length. Fe length to width ratio is 4.54, Pa 2.5, and Ti 3.

Male bulb T slender, spindle-shaped, 0.57 long and 0.25 mm wide in the widest part (bulge) (Figs 18–19). Internal T side oriented away from the palp, distally with a mild, bulge like expansion. External T side evenly rounded and facing palpal Ti. T distally flattened. Internal side of the flattened area membranous and corresponds to terminal haemethodoca from which the embolic division emerges. MA emerges from the internal side of the tegulum (Figs 18–20), below the bulge and just above the terminal haemethodoca; shaped like a weakly curved rod with a tip pointed distally; E emerging from the distal rim of terminal haemethodoca (Figs 18–19, 21–22); flat, broad, partly membranous on the edges with embolus opening on the distal rim (Fig. 22). C emerging from the middle of terminal haemethodoca, between the MA and E (Figs 18–22); slender, tapering towards the end, with a tip in the shape of a bird's head from a lateral view (Figs 18–19). Before the





**Figs. 13–14.** *Harpactea salvatorei* sp. nov. female vulva. 13. Dorsal view; 14. Ventral view. Scale bars = 0.1 mm. Abbreviations: AC, anterior arc; PD, posterior diverticulum; R, receptaculum; S, spermatheca; TB, transversal bar.



**Figs. 15–17.** *Harpactea damini* sp. nov. male habitus. 15. Prosoma, dorsal view; 16. Prosoma, ventral view; 17. Chelicerae, ventral view. Scale bars = 1 mm (15, 16); 0.25 mm (17). Abbreviations: PT, promarginal teeth; RT, retro-marginal teeth.



**Figs. 18–20.** *Harpactea damini* sp. nov. male bulb. 18. Prolateral view; 19. Retrolateral view; 20. Ventral view. Scale bars = 0.25 mm. Abbreviations: C, conductor; E, embolus; MA, median apophysis; T, tegulum.



tip there is a rounded bump while the tip is hooked-shaped and with serrated outer border (Fig. 23). MA, C, and E are all directed away from the palp. In distal view E is positioned prolaterally, MA retrolaterally and C between them. PA absent.

Female paratype CBSS/AR 4293-1. Measurements: CL, 3; Cwmax, 2.22; Cwmin, 1.37; OL, 4.05; ChL, 1.31; ChG, 0.38; ChF, 0.7; AMEd, 0.15; PLEd, 0.11; PMEd, 0.1. Leg measurements of paratype (♀): Fe I, 3; Fe II, 2.65; Fe III, 2.1; Fe IV, 3.05; Pa I, 2; Pa II, 1.75; Pa III, 1.05; Pa IV, 1.3; Ti I, 2.7; Ti II, 2.5; Ti III, 1.75; Ti IV, 2.7; Mt I, 2.5; Mt II, 2.35; Mt III, 2.3; Mt IV, 3.25; Ta I, 0.7; Ta II, 0.65; Ta III, 0.6; Ta IV, 0.75. Somatic characters as in male, except: labium length 0.72, width 0.33 mm; clypeus height 0.1 mm; relative leg lengths: IV > I > II > III; spine pattern on posterior Fe less regular (breaking the two lines organization), posterior Ti and Me with 16 and 10–14 spines respectively.

Vulva AC triangular in ventral view with frontal border heavily sclerotized (Figs 24–25). Strongly sclerotized S, base triangle-shaped, projected frontally from AC, bearing an oval-shaped top with transparent dorso-frontal SK. RS positioned laterally on AC, just before bifurcated lateral edges – dorsal one slightly bent frontally, ventral one posteriorly (Fig. 26). TB simple, slightly convex in frontal direction. PD small and poorly sclerotized round-shaped sac (Fig. 24).

**Intraspecific variation.** For the rest of the paratype material (4 females and 3 males) main body measurements were taken: males: CL, 2.7–3.38; Cwmax, 2.15–2.7; OL, 3.31–4.22; females: CL, 2.43–3.43; Cwmax, 1.81–2.4; OL, 3.06–4.57. Length variability of leg segments of I and IV legs was also measured: males: Fe I, 2.85–3.52; Fe IV, 2.78–3.61; Pa I, 1.86–2.36; Pa IV, 1.26–1.57; Ti I, 2.62–3.4; Ti IV, 2.65–3.14; Mt I, 2.9–3.35; Mt IV, 3.05–3.93; Ta I, 0.7–0.86; Ta IV, 0.73–0.97; females: Fe I, 2.29–3.2; Fe IV, 2.43–3.3; Pa I, 1.49–2.05; Pa IV, 1.07–1.52; Ti I, 2.00–3.16; Ti IV, 2.15–3.21; Mt I, 1.92–2.77; Mt IV, 2.48–3.57; Ta I, 0.51–0.71; Ta IV, 0.74–0.83. Leg spination proved to be a very variable character. In males, anterior Fe can have 10–15 spines which can be distributed all along the dorsal side. Posterior Fe with up to 16 spines deviating from the two-line organization. Posterior Ti and Me with up to 24 and 21 spines respectively. In females, anterior Fe can be with 3 to 7 spines which can be organized in a line (not clustered), Fe III and IV in one female with 5 and 4 spines respectively, and posterior Ti with 12 to 18 spines. In male pedipalps, Fe length to width ratio is between 4.14 and 4.67, Pa 2.48 to 3.54 and Ti up to 3.56.

**Distribution and ecology.** The species is known from eight caves, seven on Biokovo Mtn (separated by 20 km) and one on the slopes of Mosor Mtn, 35 km in the north-west direction from the closest Biokovo Mtn cave (Fig. 40). The caves are distributed from 338–793 m asl. All except the one on Mosor Mtn, which is 95 m deep and has a constant temperature of 7.4 °C, are relatively small and shallow caves (4–40 m deep and 19–260 m long) which seem to be influenced by outside conditions a great deal. Yearly temperature variation in all of them is huge, for example in the type locality, Jujnovića špilja, temperature measured in April was 6.3 °C and in June 13.8 °C. Similar situation is in all other caves indicating that *Harpactea damini* sp. nov. can tolerate a relatively wide range of temperatures. Given the porosity of karst landscape it is reasonable to assume that during the unfavourable conditions (in several caves temperatures measured in January were close to 0 °C and no spiders were collected) spiders migrate to the surrounding system of crevices where the micro-climatic conditions are more stable. Because of all of this, and its mild troglomorphic morphology we conclude that *Harpactea damini* sp. nov. is a troglophile.

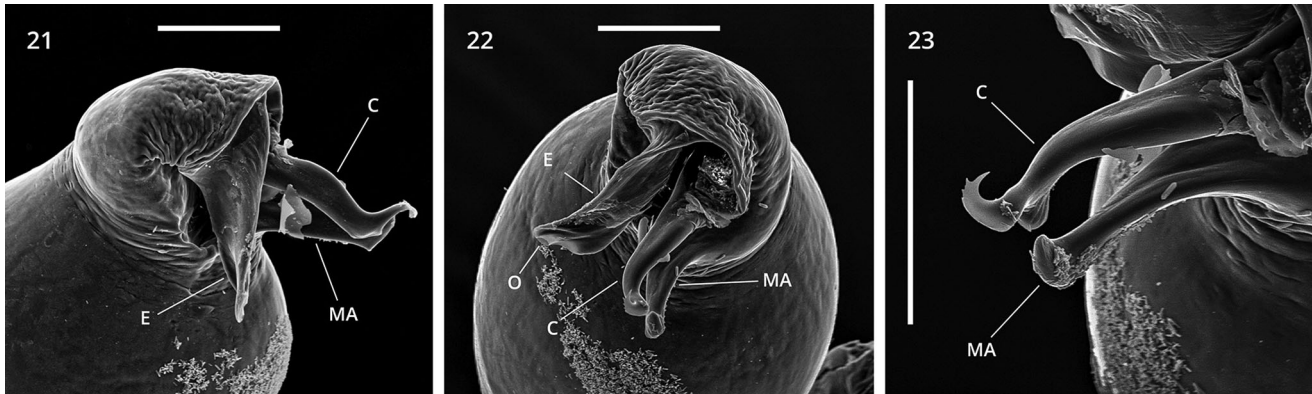
*Harpactea mateparlovi* Pavlek & Arnedo sp. nov.  
(Figs 27–38)

**Type specimens.** HOLOTYPE: 1♂ CBSS/AR 5568, Croatia, Biokovo Mtn, Biokovka, 43.32°N, 17.05°E, 22.VI.2017, leg. Jana Bedek. Deposited at CBSS. PARATYPES: 1♀ CBSS/AR 5089, Croatia, Biokovo Mt, Jama pod Kamenitim vratima, HR01919, 43.30°N, 17.12°E, 31.V.2017., leg. Teo Delić. 1♂ CBSS/AR 704, Biokovo Mt, Tučepka vilenjača, 43.29°N, 17.08°E, 9.4.1990., leg. Roman Ozimec. All samples above deposited at CBSS. 1♂ MZB 2019-2015, Croatia, Biokovo Mtn, Kuna špilja, 42.51°N, 18.37°E, 27.VIII.1998., leg. Roman Ozimec. Deposited at MCNB.

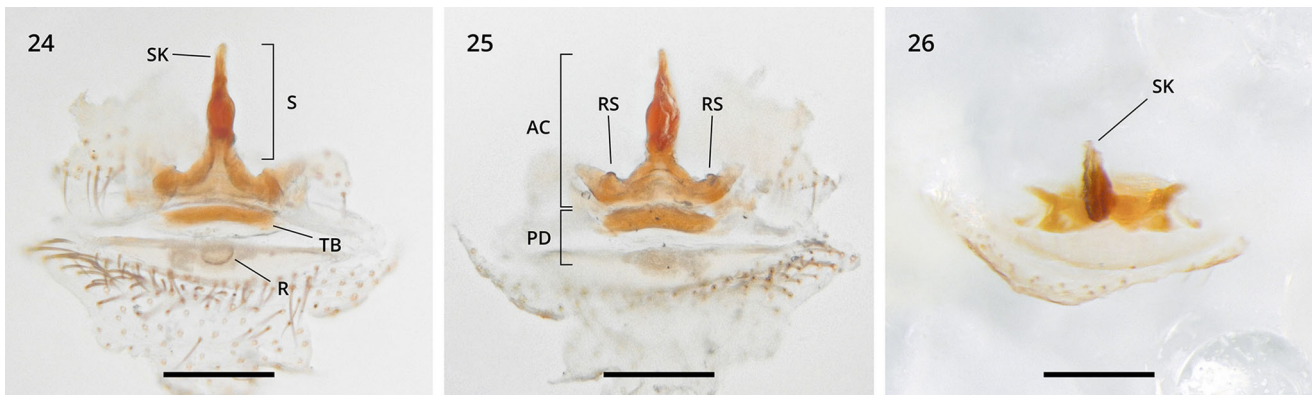
**Other material examined.** One juvenile CBSS/AR 5578, Croatia, Biokovo Mtn, Biokovka, 22.VI.2017., leg. Tamara Čuković. Deposited at CBSS.

**Type locality.** Croatia, Biokovo Mtn, Biokovka. Biokovka is almost a completely vertical, 363 m deep pit, and it already is a type locality for a carabid beetle *Derossiella lukici* Lohaj & Delić, 2019.

**Etymology.** The species is named after Mate Parlov (1948–2008), Croatian boxer, Olympic gold medallist,



**Figs. 21–23.** *Harpactea damini* sp. nov. male bulb SEM images. 21. Prolateral view; 22. Ventral view; 23. C and MA detail. Scale bars = 0.1 mm. Abbreviations: C, conductor; E, embolous; MA, median apophysis; o, sperm outlet.



**Figs. 24–26.** *Harpactea damini* sp. nov. female vulva. 24. Ventral view; 25. Dorsal view; 26. Frontal view. Scale bars = 0.2 mm. Abbreviations: AC, anterior arc; PD, posterior diverticulum; R, receptaculum; RS, oundishstructure; S, spermatheca; SK, permathecal keel; TB, transversal bar.

and European and World Champion, because of its ‘puffy’ and ‘strong’ pedipalp segments.

**Diagnosis.** Males easily recognizable by robust pedipalps with ‘puffy’ segments (Figs 27–28, 30–31). Male bulb resembles *H. complicata*, *H. lazarovi*, and *H. tenuimboli*. It is distinguished by flat, fan-shaped C (Figs 30–31, 33–35), while in the other three species C is chisel, spine or lanceolate shaped; straight, not bent, PA (Figs 30–31), which is hook shaped in *H. complicata* and *H. lazarovi*; MA with a bifurcated tip; E wavy in shape, with a pointed tip (Figs 30–35). Vulva AC with rounded lateral edges, single RS positioned dorsally, at S base; S rod-like stalk, distally round shaped, transparent ventral SK; R sclerotized, short, tube-like in lateral view, elongated laterally in dorsal view (Figs 36–38).

**Description.** 0Male holotype. Measurements: CL, 3.28; Cwmax, 2.26; Cwmin, 1.03; OL, 3.85; ChL, 1.05; ChG, 0.3; ChF, 0.49; AMEd, 0.14; PLEd, 0.13; PMEd, 0.12.

Carapace with smooth surface, light brown, darker on the edges (Fig. 27). Outline rounded with straight posterior border. Several long setae in the eyes region and very short ones on the posterior carapace edge. Fovea visible, longitudinal. Eyes clustered closely together and slightly elevated. Posterior eyes recurved, relative eyes size  $AME > PLE > PME$ ; AME separated by 1/3 of their diameter, others touching each other. Clypeus height 0.03 mm. Sternum shiny, 1.77 mm long, the same colour as carapace with scarce short setae (Fig. 28). Labium length 0.6, width 0.3 mm. Chelicerae the same colour as front part of carapace; cheliceral groove armed with 4 teeth. Two teeth on the promargin equal in size, 0.03 long and 0.03 mm wide, positioned proximally and almost touching each other. Two on the retromargin separated by 0.08 mm. Proximal-most tooth on retromargin opposite to the interspace of the two on the promargin, and half their size. Distal-most on the retromargin of the same size as the two on the promargin (Fig. 29). Cheliceral groove dorsally covered with



**Figs. 27–29.** *Harpactea mateparlovi* sp. nov. male habitus. 27. Prosoma, dorsal view; 28. Prosoma, ventral view; 29. Chelicerae, ventral view. Scale bars = 1 mm (27, 28); 0.5 mm (29). Abbreviations: PT, promarginal teeth; RT, retro-marginal teeth.

long setae, arranged in two lines. Opisthosoma light grey.

Leg measurements: Fe I, 2.55; Fe II, 2.27; Fe III, 1.94; Fe IV, 2.26; Pa I, 1.79; Pa II, 1.43; Pa III, 0.95; Pa IV, 1.31; Ti I, 2.15; Ti II, 1.82; Ti III, 1.38; Ti IV, 2.1; Mt I, 2.14; Mt II, 1.95; Mt III 1.85; Mt IV, 2.84; Ta I, 0.58; Ta II, 0.56; Ta III, 0.58; Ta IV, 0.65. All legs light brown. Ta with 3 claws. Relative leg length:  $I > II > IV > III$ . Spines present on all Fe and the posterior Ti and Me; all Cx, Pa and Ta spineless. Fe I with 8 pl spines clustered distally and Fe II with 4 pl spines arranged in one line going from the middle to the apical part. Fe III with 5–7 dorsal spines arranged in two longitudinal rows stretching along the whole length and Fe IV with 8 spines – 1 apical rl, others dorsal, in two proximal rows. Posterior Ti and Me with 11–16 and 11–17 spines respectively, distributed along the segments.

Palps the same colour as legs. All segments almost straight, and all except Fe with unequal diameter along the length. Fe 1.26 mm long, Pa 0.63 and Ti 0.7. Fe 0.39 mm wide, Pa 0.27 and Ti 0.31 mm in their widest parts. Fe length to width ratio is 3.23, Pa 2.33 and Ti 2.26. Setae present on all segments – scarce on Fe and dense on all other segments, short on dorsal and longer on the ventral side.

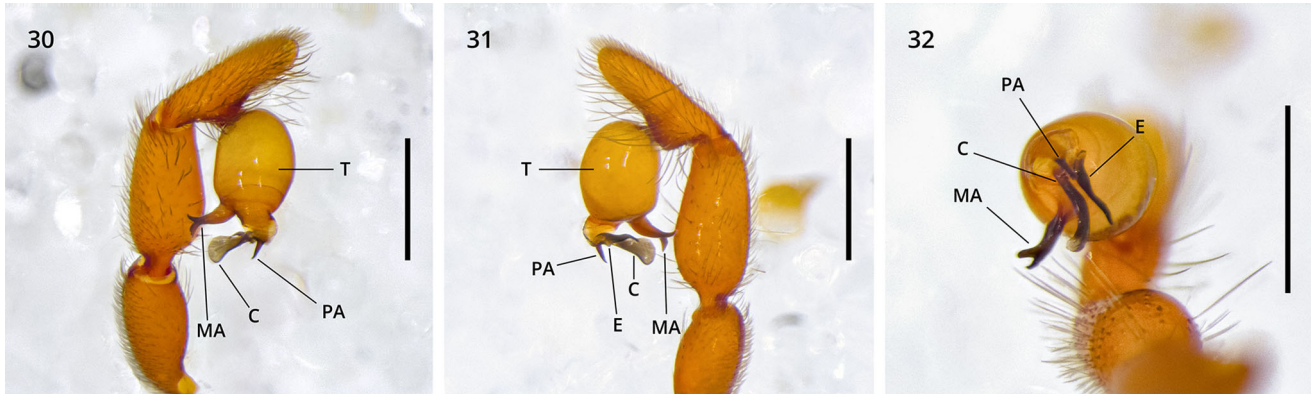
Male bulb T round-shaped, 0.53 mm long and 0.36 mm wide in the widest part which forms a bulge (Figs 30–31). Internal T side faces palpal Ti, distally with a bulge, more pronounced than in *H. damini* sp. nov. External T side evenly rounded and oriented away from the pulp. T distally flattened with terminal haemathodoca on the internal side (Fig. 31). MA emerges below the bulge, above the terminal haemathodoca, thick at the base, thinning towards the tip which is bifurcated in dorso-ventral direction (Figs 30–31, 35). PA emerges from the distal tip of flattened tegulum part

(Fig. 30), is in the shape of a short, flat, rectangular rod with broader tip (Fig. 34). E emerges from the rim of the terminal haemathodoca, wavy in shape, with embolus opening on a pointed tip (Figs 31–33). C also emerges from the terminal haemathodoca but more interiorly, between the MA and E (Figs 32, 34–35), flat, thinner at the base and widening towards the tip which is in the shape of a hand fan gently bend towards MA (in distal view). PA, MA, E and C all facing the palpal Ti. In distal view MA is positioned prolaterally, E retro-laterally and C and PA between them (Fig. 32).

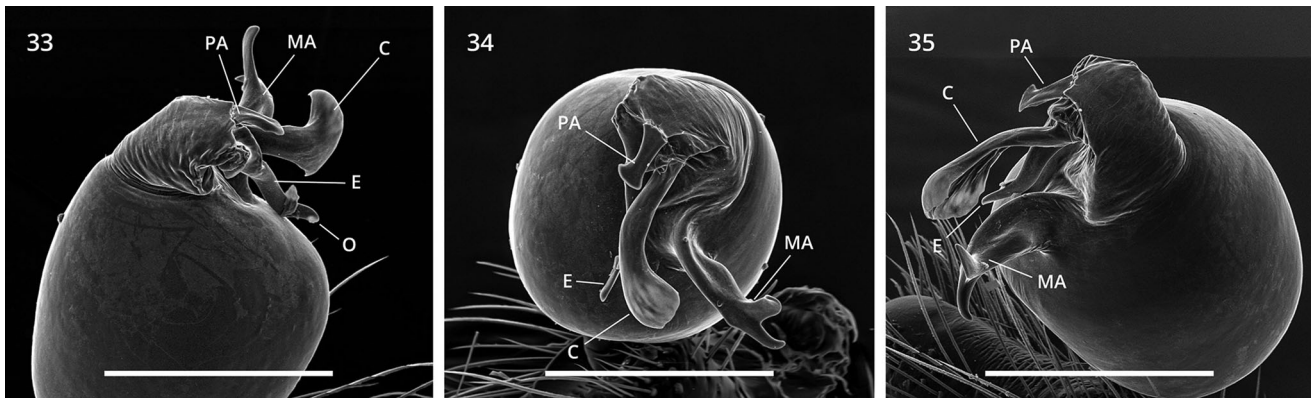
Female. Measurements: CL, 3.08; Cwmax, 2.66; Cwmin, 1.3; OL, 5.75; ChL, 1.41; ChG, 0.39; ChF, 0.72; AMEd, 0.15; PLEd, 0.15; PMEd, 0.13. Leg measurements of paratype (♀): Fe I, 2.82; Fe II, 2.6; Fe III, 2.04; Fe IV, 2.46; Pa I, 1.76; Pa II, 1.41; Pa III, 0.98; Pa IV, 1.41; Ti I, 2.46; Ti II, 2.11; Ti III, 1.62; Ti IV, 2.46; Mt I, 2.32; Mt II, 2.11; Mt III 2.18; Mt IV, 2.81; Ta I, 0.63; Ta II, 0.56; Ta III, 0.56; Ta IV, 0.77. Somatic characters as in male, except: on cheliceral groove both teeth on retromargin half the size of the two on the promargin; labium length 0.63, width 0.38 mm; relative leg lengths:  $I > IV > II > III$ ; spine pattern: Fe I with 5 to 6 and Fe II with 3–4 spines organized like in males.

Vulva AC broad with rounded lateral edges bend in dorsal direction (Figs 36–37). Strongly sclerotized S, shaped as rod-like stalk of even width, slightly dorsally inclined, bearing a round tip with transparent ventral SK. When viewed from the side, the S tip resembles a pelican's head. Single RS, positioned in the middle of the dorsal side of AC, at the base of a S. TB broader and more sclerotized posteriorly, narrower towards the tips. R sclerotized, short, tube-like in lateral view, directed ventrally. In ventral view, elongated laterally, in the shape of a smooth angled trapezoid.





**Figs. 30–32.** *Harpactea mateparlovi* sp. nov. male bulb. 30. Prolateral view; 31. Retrolateral view. 32. Ventral view. Scale bars = 0.5 mm. Abbreviations: C, conductor; E, embolous; MA, median apophysis; PA, paramedian apophysis; T, tegulum.



**Figs. 33–35.** *Harpactea mateparlovi* sp. nov. male bulb SEM images. 33. Prolateral view; 34. Ventral view; 35. Bulb detail. Scale bars = 0.3 mm. Abbreviations: C, conductor; E, embolous; MA, median apophysis; o, sperm outlet; PA, paramedian apophysis.

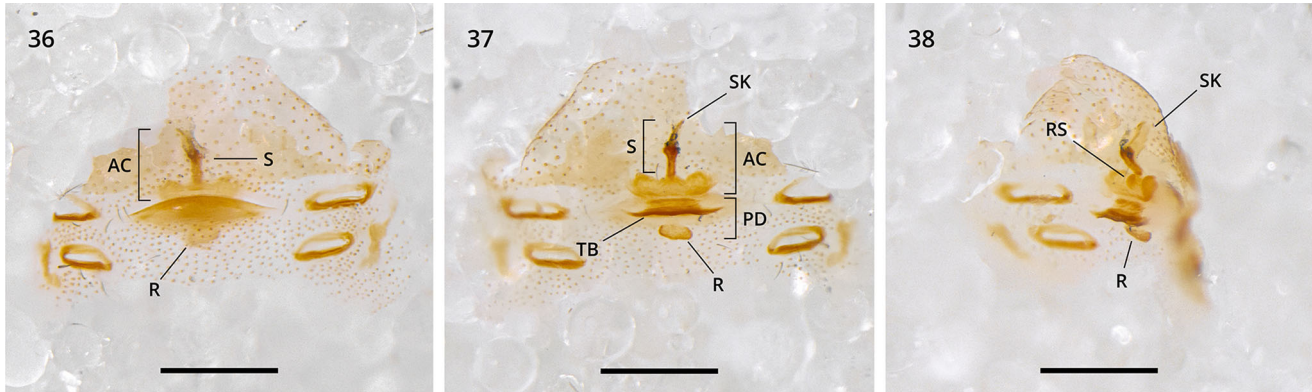
**Intraspecific variation.** For the rest of the paratype material (2 males) main body measurements were taken: CL, 2.87–3.37; Cwmax, 2.21–2.32; OL, 3.01–3.35; . Length variability of leg segments of I and IV legs was also measured: Fe I, 2.61–3.07; Fe IV, 2.75–2.76; Pa I, 1.83–1.9; Pa IV, 1.23–1.44; Ti I, 2.15–2.29; Ti IV, 2.29–2.33; Mt I, 2.39–2.42; Mt IV, 2.75–2.76; Ta I, 0.59–0.61; Ta IV, 0.74–0.85. Leg spination varies a lot: Fe I with 5 to 9 pl apical spines, Fe II with 3 to 6 spines in one pl line, Fe III with less regular spine organization, Fe IV with 5 to 7 spines, always one rl apical and the rest in two proximal dorsal rows. Posterior Ti and Me with up to 19 spines. In male pedipalps, Fe length to width ratio is between 3.13–3.24, Pa up to 2.44 and Ti 2.2–2.27. Also, the bulb can be rotated in relation to Ta up to 90° 'outward', making tegulum bulge and embolic division elements (PA, MA, E and C) directed in retrolateral direction and not posteriorly as in holotype.

**Distribution and ecology.** The species is known from four caves on Biokovo Mtn (Fig. 40), all located at

more than 1100 m asl. The caves are 6 km apart. Two of them, Biokovka and Jama za Kamenitim vratima, are vertical shafts with pitch-ramp morphology, 363 and 499 m deep respectively, with temperatures between 3.8 and 5 °C (Glavaš, 2007; Sudar *et al.*, 2017). The other two caves, Tučepška vilenjača and Kuna špilja, are smaller, 20 and around 30 m in length and with temperatures of 9.7 and 4.5 °C respectively. We consider *Harpactea mateparlovi* sp. nov. to be a troglophile species.

### Phylogenetic analyses

Results of the phylogenetic analyses are summarized in Fig. 39. All analyses recovered *Harpactea* as polyphyletic. The *lepida* and *corticalis* were the only species groups retrieved as monophyletic, albeit with low support in the first case and with a poor sampling in the second. The new species described here were supported as being part of the *lepida* group, and *H. damini* sp. nov. was inferred to be the sister species to the remaining species. All analyses recovered the paraphyly of the



**Figs. 36–38.** *Harpactea mateparlovi* sp. nov. female vulva. 36. Ventral view; 37. Dorsal view; 38. Lateral view. Scale bars = 0.5 mm. Abbreviations: AC, anterior arc; PD, posterior diverticulum; R, receptaculum; RS, roundish structure; S, spermatheca; SK, spermathecal keel; TB, transversal bar.

*hombergi* species group and supported the inclusion of the two sampled species of this group in a clade including also the *corticalis* species. All analyses recovered the polyphyly of the *rubicunda* group and provided high support for a clade including the representatives of the *rubicunda* group together with the species sampled in the genus *Dasumia* and *Minotauria*. Model based analyses also suggested paraphyly of the subfamily Harpacteinae, since the genus *Kaemis* and *Sardostalita* were more closely related to the subfamily Dysderinae. The other two subfamilies, namely Dysderinae and Rhodinae, were supported as monophyletic.

## Discussion

We provide for the first time quantitative evidence for the long time suspected polyphyly of the genus *Harpactea*. Our results clearly call for a redefinition not only of *Harpactea*, but of most current genera within Harpacteinae. This task will most likely involve the erection of new genera to accommodate some of the monophyletic groups here recovered. Unfortunately, because of the relatively modest sampling, a formal proposal for a redelimitation of *Harpactea* and its allies is beyond the scope of the present study. However, some emerging patterns are worth discussing. Our phylogeny indicates that the relatively homogeneous yet very diverse group *corticalis*, mostly circumscribed to the Western Mediterranean, renders the group *hombergi* paraphyletic. The group *hombergi*, named after the type species of *Harpactea*, is not so diverse – eight species according to Deeleman-Reinhold (1993) although species described after her work may actually belong to this complex. With the exception of the type species, the *hombergi* group is mostly confined to the Balkans. The other two groups, *lepida* and *rubicunda*, are not

closely related to the *hombergi*+*corticalis* group, albeit support for some of the basal relationships in our analyses was low. The group *rubicunda* is polymorphic and may include distinct lineages, some of which may deserve genus status on their own. However, and as already advanced by Deeleman-Reinhold (1993), several species currently assigned to *Harpactea* are indeed more closely related to *Dasumia* species. A less restrictive definition of *Dasumia* could easily accommodate these *Harpactea* species to circumscribe a natural group. On the other hand, the taxonomic circumscription of the species of the group *lepida*, which are here recovered as monophyletic albeit with low support, will most likely require the erection of a new genus. However, a more thorough species sampling will be necessary to establish the boundaries and define the traits of the new genus. The three newly described *Harpactea* species, *H. salvatorei* sp. nov., *H. damini* sp. nov., and *H. mateparlovi* sp. nov., add to the 14 species currently in *lepida*, namely *H. apollinea* Brignoli, 1978, *H. bulgarica* Lazarov & Naumova, 2010, *H. complicata* Deltchev, 2011, *H. deltchevi* Dimitrov & Lazarov, 1999, *H. grisea* (Canestrini, 1868), *H. lazarevi* Deltchev, 2011, *H. lepida* (C. L. Koch, 1838), *H. mentor* Lazarov & Naumova, 2010, *H. petrovi* Lazarov & Dimitrov, 2018, *H. simovi* Deltchev & Lazarov, 2018, *H. stoevi* Deltchev & Lazarov, 2018, *H. tenuimboli* Deltchev, 2011, *H. tergestina* Gasparo, 2014, and *H. thaleri* Alicata, 1966.

As in the remaining species groups proposed in the literature, delimitation of the *lepida* group is based on genitalic traits (Alicata, 1966; Brignoli, 1978; Deeleman-Reinhold, 1993). According to Deeleman-Reinhold (1993), the *lepida* group male bulb bears a lamella shaped C, and an apical, reflexed E, while in females the integument margins posterior to the genital slit are chitinized, the vulva PD is wider than long and bears a slightly sclerotized button (R). Additionally, the

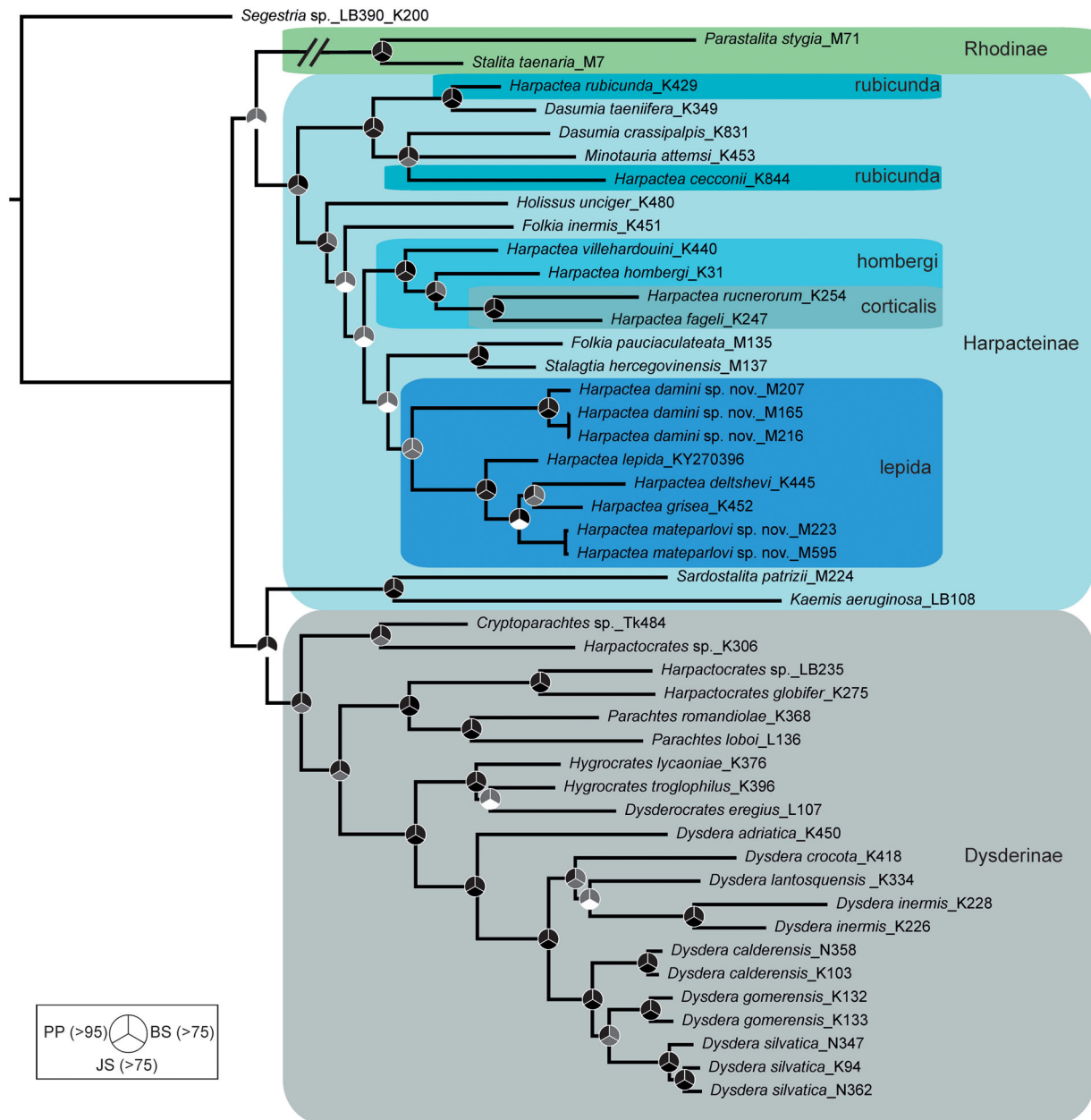


**Fig. 39.** MrBayes tree from concatenated analysis of five markers. Circles on internal nodes denote support values, as marked on the symbol in the lower left corner: PP, Bayesian posterior probability; BS, Maximum likelihood bootstrap; JC, parsimony jackknife support. Colour coding: black = PP > 95%, BS and JS > 75; grey = clades recovered with support values below the former threshold; white = clades not recovered.

Cx and Pa are spineless. The reinterpretation of some of the sclerites of the male bulb lead us to propose that the presence of a well-developed MA is shared by all the species examined and may constitute an additional diagnostic trait.

Within the *lepida* group, the female characters are either conserved or difficult to interpret. Male palp traits on the other hand are more variable and allow to put forward some hypotheses about internal relationship

between species. Species on the *lepida* group can be readily separated into two subgroups based on the presence or absence of a well-developed PA. The shared presence of a well-developed PA, along with a spiny-like E, group together the species *H. bulgarica*, *H. lazaro*vi, and *H. mentor* and three species so far only found in Dinaric and western Serbia caves, namely *H. complicata* and *H. tenuemboli*, from Serbia, and *H. mateparlovi* sp. nov. from Croatia. Among the species that lack



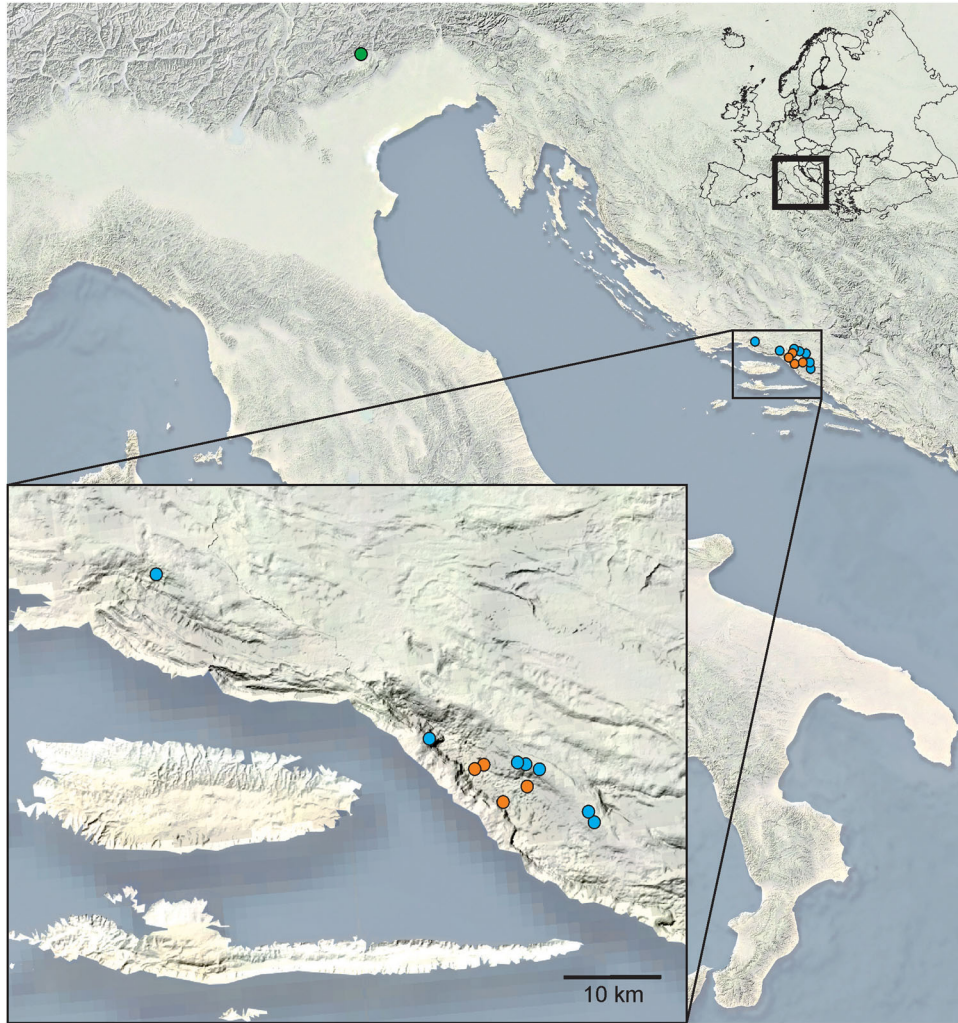


**Fig. 40.** Distribution map of *Harpactea salvatorei* sp. nov. (green circle), *Harpactea damini* sp. nov. (blue circles) and *Harpactea mateparlovi* sp. nov. (orange circles).

PA, the unique presence of a projection on the palpal patella suggests a close relationship between *H. grisea*, *H. tergestina*, and *H. salvatorei* sp. nov., which is further supported by a poorly developed, spine-like C in the three species. Possibly related to this subgroup are other species that, as the previous ones, present similar transformations on the embolar division of the bulb, including the spine-like C closely associated to a lamellar E. These species would include *H. apollinea*, *H. damini* sp. nov., *H. lepida*, and *H. thaleri*. The lamellar aspect of the terminal part of the embolic division could further relate the species *H. petrovi* and *H. deltshevi*, which share a unique fusion of most of the structures of the embolic division with the exception of the distal part of the embolus, to the former species. The species *H. stoevi* and *H. simovi*, like the species discussed above, also lack an obvious PA and both share a spine-

like E. Additionally, similar to the species from the Alps, they both bear a spine-like C.

The *lepida* group seems to be mostly circumscribed to the eastern Alps and the Balkans. One species, *H. lepida*, is widespread in central and southern Europe, from France to Ukraine, while all other species have narrow distributions. The group with well-developed PA is restricted to the Balkans, specifically Bulgaria, Serbia, and Croatia (Fig. 40). The group of species lacking the PA is more broadly distributed. Interestingly, the three species with palpal patellar projection, including *H. salvatorei* sp. nov. (Fig. 40), as well as two species without patellar modification but similar transformations of the embolar division, namely *H. thaleri* and *H. lepida*, are either circumscribed to or found (*H. lepida*) in the Alps. Of the remaining members of the group lacking PA, *H. apollinea* and *H.*

*damini* sp. nov. (Fig. 40) are distributed in the southern Balkans, while the others are confined to eastern Balkans, specifically to Bulgaria.

According to Mammola et al. (2018) and Gücel et al. (2019), there are 19 *Harpactea* species with some level of somatic adaptation to the underground environment. Four species have no trace of eyes and are considered true troglobites while the remaining species show different levels of eye reduction and depigmentation, and are better considered troglomorphic (Mammola et al., 2018). We consider the three newly described species as troglomorphic, raising the number of cave-dwelling *Harpactea* species to 22.

In this study, we have provided the first quantitative phylogenetic evidence of the largely suspected polyphyly of the species-rich genus *Harpactea*, and have put forward some groupings, and discuss their defining traits, that could provide the foundations of a more natural taxonomy of the lineage. A more thorough taxonomic sampling and a larger amount of molecular data will be necessary to successfully infer a fully resolved phylogeny of the genus and its relatives, which will allow testing the trait homologies here proposed and formally describe the new groupings.

## Acknowledgements

Sincere thanks to Giuliano Trezzi, Christa Deeelman-Reinhold, Peter Hlaváč, Jan Lakota, David Čeplik, and all members of CBSS who collected the spider material, to Fulvio Gasparo, who loaned us the samples of *H. grisea* and *H. tergestina* used for the comparison, to Adrià Bellvert and Luis Crespo of the Arnedo Lab group, for the help with the microscopes and vulva preparation, to Humbert Salvadó for granting access to the optical microscope and to Giorgio Fornasier for providing the bibliography of the Italian cave. Thanks to Tin Rožman for help in adjusting photos and figures. We are most grateful to Stefano Mammola (Verbania, Italy), Robert (Bob) J. Kallal (Washington DC, USA) and an anonymous reviewer for their insightful comments on earlier versions of the manuscript.

## Disclosure statement

No potential conflict of interest was reported by the authors.

## Supplemental data

Supplemental data for this article can be accessed here: <https://doi.org/10.1080/14772000.2020.1776786>.

## Funding

The work was financially supported by a Marie Skłodowska-Curie Individual Fellowship (749867) (MP), Agència de Gestió d'Ajuts Universitaris i de Recerca (<http://agaur.gencat.cat/en/inici/>), and by CGL2016-80651-P from the Spanish Ministry of Economy and Competitiveness (MA) and 2017SGR83 from the Catalan Government (MA).

## ORCID

Martina Pavlek  <http://orcid.org/0000-0001-6710-0581>

Miquel Arnedo  <http://orcid.org/0000-0003-1402-4727>

## References

- Alicata, P. (1966). Le *Harpactea* (Araneae, Dysderidae) della fauna italiana e considerazioni sulla loro origine. *Atti Dell'Accademia Gioenia Di Scienze Naturali in Catania*, 6(18), 190–221.
- Arnedo, M. A., Oromi, P., Murria, C., Macias-Hernandez, N., & Ribera, C. (2007). The dark side of an island radiation: Systematics and evolution of troglomorphic spiders of the genus *Dysdera* Latreille (Araneae: Dysderidae) in the Canary Islands. *Invertebrate Systematics*, 21(6), 623–660. <https://doi.org/10.1071/IS07015>
- Arnedo, M., Gasparo, F., & Opatova, V. (2009). Systematics and phylogeography of the *Dysdera erythrina* species complex (Araneae, Dysderidae) in Sardinia. *ZooKeys*, 16, 319–345. <https://doi.org/10.3897/zookeys.16.128>
- Arnedo, M., Oromi, P., & Ribera, C. (2001). Radiation of the Spider Genus *Dysdera* (Araneae, Dysderidae) in the Canary Islands: Cladistic Assessment Based on Multiple Data Sets. *Cladistics*, 17(4), 313–353. <https://doi.org/10.1006/clad.2001.0168>
- Astrin, J. J., Höfer, H., Spelda, J., Holstein, J., Bayer, S., Hendrich, L., Huber, B. A., Kielhorn, K.-H., Krammer, H.-J., Lemke, M., Monje, J. C., Morinière, J., Rulik, B., Petersen, M., Janssen, H., & Muster, C. (2016). Towards a DNA barcode reference database for spiders and harvestmen of Germany. *PLoS One*, 11(9), e0162624–24. <https://doi.org/10.1371/journal.pone.0162624>
- Ballarin, F., Pantini, P., & Hansen, H. (2011). Catalogo ragionato dei ragni (Arachnida, Araneae) del Veneto. *Memorie Del Museo Civico Di Storia Naturale Di Verona*, 2, 1–151.
- Belloni, S., Martinis, B., & Orombelli, G. (1971). *Karst of Italy. Karst Important Region of the Northern Hemisphere*. M. Herak and V. T. Stringfield (Eds). Elsevier Publishing Company Amsterdam.
- Bidegaray-Batista, L., & Arnedo, M. a. (2011). Gone with the plate: the opening of the Western Mediterranean basin drove the diversification of ground-dweller spiders. *BMC Evolutionary Biology*, 11(1), 317. <https://doi.org/10.1186/1471-2148-11-317>
- Bidegaray-Batista, L., Ferrández, M. Á., & Arnedo, M. A. (2014). Winter is coming: Miocene and Quaternary climatic shifts shaped the diversification of Western-Mediterranean Harpactocrates (Araneae, Dysderidae) spiders. *Cladistics*, 30(4), 428–446. <https://doi.org/10.1111/cla.12054>

- Bidegaray-Batista, L., Macías-Hernández, N., Oromí, P., & Arnedo, M. A. (2007). Living on the edge: demographic and phylogeographical patterns in the woodlouse-hunter spider *Dysdera lancerotensis* Simon, 1907 on the eastern volcanic ridge of the Canary Islands. *Molecular Ecology*, 16(15), 3198–3214. <https://doi.org/10.1111/j.1365-294X.2007.03351.x>
- Bosselaers, J., & Van Keer, J. (2016). A redescription of *Harpactea dufouri* (Thorell, 1873) (Araneae, Dysderidae), its occurrence outside the Balearic Islands, and some notes on the corticalis group of the genus. *European Journal of Taxonomy*, 222(222), 1–13. <https://doi.org/10.5852/ejt.2016.222>
- Brignoli, P. M. (1978). Ragni di Turchia V. Specie nuove o interessanti, cavernicole ed epigee, di varie famiglie (Araneae). *Revue Suisse de Zoologie*, 85, 461–541. <https://doi.org/10.5962/bhl.part.82243>
- Burger, M., & Kropf, C. (2007). Genital morphology of the haplogyne spider *Harpactea lepida* (Arachnida, Araneae, Dysderidae). *Zoomorphology*, 126(1), 45–52. <https://doi.org/10.1007/s00435-007-0029-1>
- Chatzaki, M., & Arnedo, M. A. (2006). Taxonomic revision of the epigean representatives of the spider subfamily Harpactinae (Araneae: Dysderidae) on the island of Crete. *Zootaxa*, 1169(1), 1–32. <https://doi.org/10.11646/zootaxa.1169.1.1>
- Corrado, C. (1953). Le Grotte della bassa Valcellina. *Riv. Mens. C.A.I.*, 72(11/12), 367–372.
- Deeleman-Reinhold, C. L. (1993). The genus *Rhode* and the harpactine genera *Stalagtia*, *Folkia*, *Minotauria*, and *Kaemis* (Araneae, Dysderidae) of Yugoslavia and Crete, with remarks on the genus *Harpactea*. *Revue Arachnologique*, 10(6), 105–135.
- Deltshev, C., & Lazarov, S. (2018). Two new spider species, *Harpactea simovi* sp. n. and *H. stoevi* sp. n. (Araneae: Dysderidae), from the Balkan Peninsula. *Acta Zoologica Bulgarica*, 70, 3–7.
- Dimitrov, D., Deltshev, C., & Lazarov, S. (2019). Description of *Harpactea popovi* sp. n. from Bulgaria with further taxonomic notes on related species (Araneae, Dysderidae). *Zootaxa*, 4568(3), 593–600. <https://doi.org/10.11646/zootaxa.4568.3.13>
- Dimitrov, D., & Lazarov, S. (1999). Two new species of Harpactea from Bulgaria (Araneae: Dysderidae). *Berichte des Naturwissenschaftlich-Medizinischen Vereins in Innsbruck*, 86, 127–129.
- Forster, R. R., & Platnick, N. I. (1985). A review of the austral spider family Orsolobidae (Arachnida, Araneae), with notes on the superfamily Dysderoidea. *Bulletin of the American Museum of Natural History*, 181, 1–230.
- Gasparo, F. (1997). Miscellanea biospelologica. Parte I: Friuli. In E. Boegan, (Ed) “Atti e Memorie della Commissione Grotte, (Vol. 34, pp. 17–48). Trieste.
- Gasparo, F. (2013). Descrizione di una nuova specie del genere *Harpactea* Bristowe, 1939 del Carso Triestino (Araneae, Dysderidae). *Atti Del Museo Civico Di Storia Naturale - Trieste*, 56, 207–217.
- Gasparo, F., & Thaler, K. (2000). I ragni cavernicoli della Venezia Giulia (Italia nord-orientale) (Arachnida, Araneae). *Atti e Memorie, Commissione Grotte “Eugenio Boegan”* 37, 17–55.
- Glavaš, I. (2007). Nova istraživanja jame Biokovke u 2007. godini. *Subterranea Croatica*, 9, 13–16.
- Goloboff, P. A., & Catalano, S. A. (2016). TNT version 1.5, including a full implementation of phylogenetic morphometrics. *Cladistics*, 32(3), 221–238. Retrieved from <http://www.lillo.org.ar/phylogeny/tnt/> <https://doi.org/10.1111/cla.12160>
- Grottolo, M. (1994). Note complementari su *Orotrechus schwiebneri* Gottolo e Martinelli, 1991 (Coleoptera Carabidae Trechinae). «*Natura Bresciana*» *Ann. Mus. Civ. Se. Nat., Brescia*, 29(1993), 185–192.
- Gücel, S., Charalambidou, I., Göçmen, B., & Kunt, K. B. (2019). New data of spiders (Arachnida, Araneae) of Cyprus. 1. Dysderidae found in caves. *ZooKeys*, 825, 43–53. <https://doi.org/10.3897/zookeys.825.29029>
- Hlaváč, P., Bregović, P., & Jalžić, B. (2019). Endogean and cavernicolous Coleoptera of the Balkans. XVIII. Strong radiation in caves of the Central Dinarides: seven new species of *Thaumastocephalus* Poggi et al., 2001 (Staphylinidae: Pselaphinae). *Zootaxa*, 4559(1), 90–110. <https://doi.org/10.11646/zootaxa.4559.1.3>
- Kalyaanamoorthy, S., Minh, B. Q., Wong, T. K. F., Von Haeseler, A., & Jermini, L. S. (2017). ModelFinder: Fast model selection for accurate phylogenetic estimates. *Nature Methods*, 14(6), 587–589. <https://doi.org/10.1038/nmeth.4285>
- Katoh, K., Misawa, K., Kuma, K., & Miyata, T. (2002). MAFFT: a novel method for rapid multiple sequence alignment based on fast Fourier transform. *Nucleic Acids Research*, 30(14), 3059–3066. <https://doi.org/10.1093/nar/gkf436>
- Kearse, M., Moir, R., Wilson, A., Stones-Havas, S., Cheung, M., Sturrock, S., Buxton, S., Cooper, A., Markowitz, S., Duran, C., Thierer, T., Ashton, B., Meintjes, P., & Drummond, A. (2012). Geneious Basic: An integrated and extendable desktop software platform for the organization and analysis of sequence data. *Bioinformatics (Oxford, England)*, 28(12), 1647–1649. <https://doi.org/10.1093/bioinformatics/bts199>
- Lanfear, R., Frandsen, P. B., Wright, A. M., Senfeld, T., & Calcott, B. (2017). Partitionfinder 2: New methods for selecting partitioned models of evolution for molecular and morphological phylogenetic analyses. *Molecular Biology and Evolution*, 34(3), 772–773. <https://doi.org/10.1093/molbev/msw260>
- Lazarov, S., & Dimitrov, D. (2018). Description of *Harpactea petrovi* sp. n. (Araneae: Dysderidae) from Bulgaria. *Acta Zoologica Bulgarica*, 70, 293–296.
- Lazarov, S., & Naumova, M. (2010). Two new Harpactea species from Bulgaria (Araneae: Dysderidae). *Revue Suisse de Zoologie*, 117, 101–110.
- Le Peru, B. (2011). The Spiders of Europe, a synthesis of data: Volume 1 Atypidae to Theridiidae. *Mémoires de La Société Linnéenne de Lyon*, 2, 1–522.
- Lohaj, R., & Delić, T. (2019). Playing hard to get: two new species of subterranean Trechini beetles (Coleoptera, Carabidae, Trechinae) from the Dinaric Karst. *Deutsche Entomologische Zeitschrift*, 66(1), 1–15. <https://doi.org/10.3897/dez.66.31754>
- Macías-Hernández, N., Oromí, P., & Arnedo, M. A. (2008). Patterns of diversification on old volcanic islands as revealed by the woodlouse-hunter spider genus *Dysdera* (Araneae, Dysderidae) in the eastern Canary Islands. *Biological Journal of the Linnean Society*, 94(3), 589–615. <https://doi.org/10.1111/j.1095-8312.2008.01007.x>



- Macías-Hernández, N., Oromí, P., & Arnedo, M. a. (2010). Integrative taxonomy uncovers hidden species diversity in woodlouse hunter spiders (Araneae, Dysderidae) endemic to the Macaronesian archipelagos. *Systematics and Biodiversity*, 8(4), 531–553. <https://doi.org/10.1080/14772000.2010.535865>
- Mammola, S., Cardoso, P., Angyal, D., Balázs, G., Blick, T., Brustel, H., Carter, J., Ćurčić, S., Danflous, S., Dányi, L., Déjean, S., Deltchev, C., Elverici, M., Fernández, J., Gasparo, F., Komnenov, M., Komposch, C., Kováč, L., Kunt, K. B., ... Isaia, M. (2019). Continental data on cave-dwelling spider communities across Europe (Arachnida: Araneae). *Biodiversity Data Journal*, 7, e38492 <https://doi.org/10.3897/BDJ.7.e38492>
- Mammola, S., Cardoso, P., Ribera, C., Pavlek, M., & Isaia, M. (2018). A synthesis on cave-dwelling spiders in Europe. *Journal of Zoological Systematics and Evolutionary Research*, 56(3), 301–316. <https://doi.org/10.1111/jzs.12201>
- Miller, M. A., Pfeiffer, W., & Schwartz, T. (2010, April 2016). *Creating the CIPRES Science Gateway for inference of large phylogenetic trees [Paper presentation]*. 2010 Gateway Computing Environments Workshop, GCE 2010, <https://doi.org/10.1109/GCE.2010.5676129>
- Mosetti, S. (1954a). Gruppo Triestino Speleologi, *Atti del VI Congr. Naz. di Spel.*, Trieste 1954: LXV-LXVI
- Mosetti, S. (1954b). Le Grotte della Valcellina, *Atti del VI Congr. Naz. di Spel.*, Trieste 1954: 310-32
- Nentwig, W., Blick, T., Bosmans, R., Gloor, D., Hänggi, A., Kropf, C. (2020). Araneae. Retrieved from <https://www.araneae.nmbe.ch>
- Nguyen, L. T., Schmidt, H. A., Von Haeseler, A., & Minh, B. Q. (2015). IQ-TREE: A fast and effective stochastic algorithm for estimating maximum-likelihood phylogenies. *Mol. Biol. Evol.*, 32(1), 268–274. <https://doi.org/10.1093/molbev/msu300>
- Pantini, P., & Isaia, M. (2019). Araneae.it: the online Catalog of Italian spiders, with addenda on other Arachnid Orders occurring in Italy (Arachnida: Araneae, Opiliones, Palpigradi, Pseudoscorpionida, Scorpiones, Solifugae). *Fragmenta Entomologica*, 51(2), 127–152. <https://doi.org/10.4081/fe.2019.374>
- Piva, E. (2005). Nuove specie di *Orostygia* e *Oryotus*, con note sinonimiche (Coleoptera Cholevidae). *Memorie Della Società Entomologica Italiana*, 84(1), 3–44. <https://doi.org/10.4081/memorieSEI.2005.3>
- Rambaut, A., Drummond, A. J., Xie, D., Baele, G., & Suchard, M. A. (2018). Posterior summarization in Bayesian phylogenetics using Tracer 1.7. *Systematic Biology*, 67(5), 901–904. <https://doi.org/10.1093/sysbio/syy032>
- Ramírez, M. J., & Michalik, P. (2019). The Spider Anatomy Ontology (SPD)—A Versatile Tool to Link Anatomy with Cross-Disciplinary Data. *Diversity*, 11(10), 202. <https://doi.org/10.3390/d11100202>
- Roewer, C.-F. (1931). Arachnoideen aus südostalpinen Höhlen gesammelt von Herrn Karl Strasser in den Jahren 1929 und 1930. *Mitteilungen Über Höhlen- Und Karstforschung*, 1931, 1–17.
- Ronquist, F., & Huelsenbeck, J. P. (2003). MrBayes 3: Bayesian phylogenetic inference under mixed models. *Bioinformatics (Oxford, England)*, 19(12), 1572–1574. <https://doi.org/10.1093/bioinformatics/btg180>
- Rucner, D., & Rucner, R. (1995). Beitrag zur Kenntnis einiger Arthropoden (Scorpiones, Pseudoscorpiones, Araneae, Acari, Diplopoda und Chilopoda) in den Waldassoziationen Kroatiens. *Natura Croatica*, 4, 185–225.
- Sudar, V., Kuharić, N., Bregović, P., & Kirin, A. (2017). Prva biospeleološka ekspedicija - Biokovo 2017. *Subterranea Croatica*, 23, 2–20.
- Wheeler, W. C., Coddington, J. A., Crowley, L. M., Dimitrov, D., Goloboff, P. A., Griswold, C. E., Hormiga, G., Prendini, L., Ramírez, M. J., Sierwald, P., Almeida-Silva, L., Alvarez-Padilla, F., Arnedo, M. A., Benavides Silva, L. R., Benjamin, S. P., Bond, J. E., Grismado, C. J., Hasan, E., Hedin, M., ... Zhang, J. (2017). The spider tree of life: Phylogeny of Araneae based on target-gene analyses from an extensive taxon sampling. *Cladistics*, 33(6), 574–543. <https://doi.org/10.1111/cla.12182>
- World Spider Catalog. (2020). World Spider Catalog. <https://doi.org/10.24436/2>

**Associate Editor: Rosa Fernandez**